

Sediment Monitored Natural Recovery Evidenced by Compound Specific Isotope Analysis and High-Resolution Pore Water Sampling

Elodie Passeport,^{*,†,‡,§,○} Richard Landis,^{‡,∇} Georges Lacrampe-Couloume,[†] Edward J. Lutz,[§] E. Erin Mack,^{||} Kathryn West,[⊥] Scott Morgan,[⊥] and Barbara Sherwood Lollar[†]

[†]Department of Earth Sciences, University of Toronto, Toronto, Ontario, M5S 3B1, Canada

[‡]DuPont Engineering and Technology, Wilmington, Delaware 19803, United States

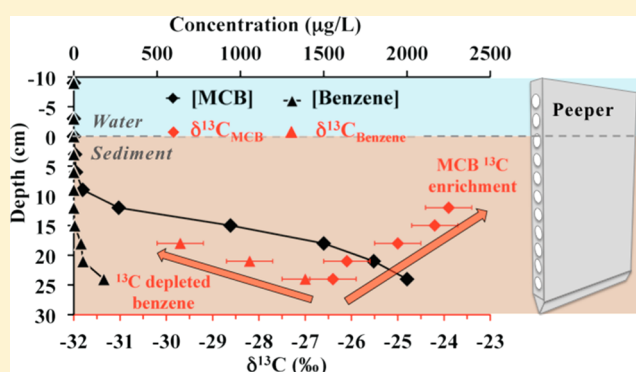
[§]The Chemours Company, Corporate Remediation Group, Wilmington, Delaware 19899, United States

^{||}DuPont Corporate Remediation Group, Wilmington, Delaware 19803, United States

[⊥]AECOM, Deepwater, New Jersey 02907, United States

Supporting Information

ABSTRACT: Monitoring natural recovery of contaminated sediments requires the use of techniques that can provide definitive evidence of in situ contaminant degradation. In this study, a passive diffusion sampler, called “peeper”, was combined with Compound Specific Isotope Analysis to determine benzene and monochlorobenzene (MCB) stable carbon isotope values at a fine vertical resolution (3 cm) across the sediment water interface at a contaminated site. Results indicated significant decrease in concentrations of MCB from the bottom to the top layers of the sediment over 25 cm, and a 3.5 ‰ enrichment in $\delta^{13}\text{C}$ values of MCB over that distance. Benzene was always at lower concentrations than MCB, with consistently more depleted $\delta^{13}\text{C}$ values than MCB. The redox conditions were dominated by iron reduction along most of the sediment profile. These results provide multiple lines of evidence for in situ reductive dechlorination of MCB to benzene. Stable isotope analysis of contaminants in pore water is a valuable method to demonstrate in situ natural recovery of contaminated sediments. This novel high-resolution approach is critical to deciphering the combined effects of parent contaminant (e.g., MCB) degradation and both production and simultaneous degradation of daughter products, especially benzene.



INTRODUCTION

Contaminated sediments are a widespread global problem. Throughout the United States, 96 out of >2,100 watersheds surveyed are considered as areas of probable concern for sediment contamination.¹ A total volume of 1.2 billion cubic yards (0.9 billion m³) of contaminated sediments, representing 10 % of the United States sediments, were estimated as sufficiently contaminated to affect aquatic organisms and human health.² Adsorbed contaminants can desorb into and partition with the sediment pore water, serving as long-term sources of dissolved contaminants to groundwater and surface waters. In the top 0–10 cm interval of sediments, often referred to as the biologically active zone, pore water concentrations are the principal exposure pathway for benthic invertebrates³ which are the first link of the food chain. The proximity to these organisms and other receptors make the sediment–water interface a critical zone on which to focus remediation efforts and assessment in contaminated sediments.⁴

Clean-up methods for contaminated sediments include in situ capping, dredging, and monitored natural recovery

(MNR).³ Monitored natural recovery relies on natural physical, chemical, and biological processes that reduce risk for ecological and human health.⁵ Field monitoring of sediment contamination, laboratory experiments, and modeling studies are needed to provide lines of evidence that MNR is actively occurring.⁵ While there are generally no construction costs involved in MNR, the extensive monitoring typically required can be expensive, especially when extrapolated over long time scales, in addition to those associated with contaminant source control. Compound Specific Isotope Analysis (CSIA) is an efficient and widely used method to monitor natural attenuation and provide insights into contaminant origin or degradation processes.⁶ Compound Specific Isotope Analysis relies on the determination of stable isotope delta values, $\delta^{13}\text{C}$,

Received: June 13, 2016

Revised: October 12, 2016

Accepted: October 22, 2016

Published: October 23, 2016

expressed in ‰, defined as the ratio between the $^{13}\text{C}/^{12}\text{C}$ ratio of a sample (R_s) and an international standard (R_{std}) (eq 1):

$$\delta^{13}\text{C} = \frac{R_s - R_{\text{std}}}{R_{\text{std}}} \quad (1)$$

Molecules containing exclusively light isotopes (e.g., ^{12}C) react faster than those incorporating one or more heavy isotopes (e.g., ^{13}C), in a process called the Kinetic Isotope Effect (KIE). During the course of degradation, the KIE results in enrichment in ^{13}C in the remaining unreacted contaminant pool. This leads to isotopic fractionation, that is, a change in overall $^{13}\text{C}/^{12}\text{C}$ for the contaminant of concern, quantified by an enrichment factor, ϵ , determined by the correlation between the fraction of remaining compound (f) at time t and stable isotope delta values defined by the Rayleigh equation (eq 2):

$$\frac{\delta^{13}\text{C} + 1}{\delta^{13}\text{C}_0 + 1} = f^\epsilon \quad (2)$$

where $\delta^{13}\text{C}$ and $\delta^{13}\text{C}_0$ are the stable isotope delta values at time t and zero, respectively.⁶

The behavior of ^{12}C - and ^{13}C -bearing compounds is typically less strongly affected by nondegradative processes such as adsorption, dissolution, volatilization, and diffusion.^{7–12} Carbon isotopic analysis has therefore made it possible to distinguish between degradative and nondegradative processes, and even to quantify the extent of contaminant degradation.⁶ To date, despite many successful applications of CSIA to contaminated groundwater (e.g., refs 13–16), it has not been extensively applied to MNR of contaminated sediments. In one of the few applications of isotope analysis to sediment environments to date, Braeckvelt (2007) collected sediment pore water samples at various locations along a wetland transect using active pore water sampling. A small enrichment in ^{13}C (approximately 1‰) was observed in monochlorobenzene (MCB) as concentrations decreased from 20 mg/L to below detection limits.¹⁷ Passive pore water sampling techniques (peepers) allow a high vertical resolution sampling across the sediment–water interface. Coupling peepers with CSIA for investigation of dissolved methane profiles has successfully elucidated the origin and transformation of methane in sediments contaminated with polycyclic aromatic hydrocarbons.^{18–20} To our knowledge, the only other use of peeper sampling in combination with isotope analysis involved stable iron isotope analysis which demonstrated the dominance of dissimilatory iron(III) reduction in an oligotrophic lake.²¹

A successful application of CSIA to sediment pore water requires the use of a sampling technique that would not affect isotope values for the target compounds. This was recently demonstrated, establishing peepers as a reliable method for CSIA for volatile organic compounds (VOCs) such as benzene, toluene, monochlorobenzene, and 1,2-dichlorobenzene.⁷

This study is the first to apply peepers and CSIA in the field to investigate the processes and effectiveness of MNR in sediments at a field site contaminated with chlorinated benzenes and benzene.

MATERIALS AND METHODS

Study Site. The study was conducted in the Salem Canal at the Chemours Chambers Works site in Deepwater, NJ. The site is a historical chemical production facility where chlorinated benzenes were used in dye manufacturing until the 1960s. This resulted in the contamination of groundwater with trichloro-

obenzenes, dichlorobenzenes, and monochlorobenzene. In 2002, the contaminated groundwater discharged into the canal sediments, where chlorinated aromatics accumulated. A sheet pile barrier was installed along the edge of the canal for physical source control and to restrict further connection between the contaminated groundwater and canal sediments. The Salem Canal sediment texture ranges from silt loam to sandy loam, with a total organic content of 2–5%.

Peeper Preparation and Deployment. The design of the peepers used in this study was described in detail in Passepport et al. (2014).⁷ Briefly, each peeper was 39.5 cm long, 20.4 cm wide, and 3.3 cm thick. Each consisted of 11 chambers distributed vertically (every 3 cm) on each side of the peeper, into which 40 mL EPA VOA vials were slotted (total of 22 vials per peeper). The 40 mL EPA VOA vials were filled with O_2 -free deionized (DI) water and covered with a 0.45 μm polysulfone membrane before insertion in the peeper body. The membrane exposed surface area for each peeper vial was 3.1 cm^2 . A Viton O-Ring was used to secure the membrane around the VOA vial neck, and another one was used to maintain the VOA vial in place in the peeper chambers. Further details and verification tests were provided in Passepport et al. (2014).⁷ The peepers containing the vials were deoxygenated for 2 days before field deployment by letting them sit in a large bucket filled with O_2 -free DI water, which was continuously bubbled with N_2 to maintain anoxic conditions in the vials. The day of field deployment, each peeper was taken out of the bucket and immediately placed in doubled plastic bags filled with N_2 to further ensure the anaerobic nature of the system. Peepers were inserted into the sediments from a boat using an installation device to push them gently into place. The peepers spent approximately 2 h in the N_2 -filled plastic bag, and were exposed to air for less than 1 min during installation. Triplicate peepers were installed side by side (50–100 cm apart) in three locations referred to as location A–B–C (peepers A, B, and C), location D–E–F (peepers D, E, and F), and location G–H–I (peepers G, H, and I). These locations were selected based on former sediment monochlorobenzene concentration data from previous monitoring rounds. One peeper from each location was used for compositional analysis of groundwater geochemical species and VOCs, and the other two were used for CSIA for the targeted VOCs. Each peeper was fitted with a rope attached to a buoy to facilitate retrieval and easily identify its location. The installation device was designed to protect the vials and avoid their membranes from being damaged during peeper insertion in the sediment. It was also designed to allow the top two vials of each peeper to be in the surface water, while the rest were in the sediment. This was done to straddle the sediment–water interface. Upon retrieval, a brown discoloration mark was used to confirm the location of the water–sediment interface. The peepers were retrieved after 4 weeks, which has been shown to allow VOC concentrations to reach equilibrium.⁷ The peepers were opened to remove the VOA vials, which were immediately capped. If residual sediment was present, DI water was used to briefly rinse the surface of the membrane before screwing the cap on. The VOA vials were placed in N_2 -filled plastic bags in a cooler filled with ice, and immediately sent to the laboratories for analysis. For each peeper, the time for peeper retrieval from the sediments, collection and capping, and placement of the peeper vials in the plastic bags was 5–10 min. At the lab for CSIA, each VOA vial was opened, the membrane removed, and 1 mL of 12N H_2SO_4 added. VOA vials were resealed quickly and kept refrigerated at

4 °C until analysis. Laboratory protocol tests have shown the compatibility of these peepers for reproducible and accurate CSIA of aromatic and chlorinated aromatic compounds dissolved in the sediment porewater.⁷

Concentration and Stable Isotope Analysis. Concentrations of nitrate, sulfate, and chloride were determined by ion chromatography following U.S. EPA method 300.0, with a limit of quantification (LOQ) < 1 mg/L and relative percentage differences (RPD) < 2 %. Total iron concentrations (LOQ = 0.2 mg/L, RPD = 4 %) were measured after acid digestion (SW 846 3010A) by inductively coupled plasma-atomic emission spectrometry (SW 846 6010B). Benzene (LOQ = 5 µg/L, RPD = 2 %) and monochlorobenzene (LOQ = 5 µg/L, RPD = 1 %) concentrations were measured by purge-and-trap (SW 846 5030B) interfaced with gas chromatography–mass spectrometry (GC/MS, method SW 846 8260B). No higher chlorinated benzenes were detected. All the analyses were done at a commercial laboratory.

Stable carbon isotope analysis was performed at the University of Toronto by gas chromatography combustion isotope ratio mass spectrometry (GC/C/IRMS) using a GC Varian 3400 and a Finnigan MAT 252, fitted with a VOCOL column (Supelco, 60 m × 0.32 mm, 3 µm film thickness). The injector temperature was 180 °C, and the temperature program started at 40 °C, held for 2 min, increased up to 175 °C at 7 °C/min, then increased up to 210 °C at 10 °C/min, held 10 min. Samples were introduced in the GC/C/IRMS by either direct headspace injections (1 mL) or, for lower concentrations, after preconcentration by purge-and-trap (P&T, Tekman Tekman Purge Trap K, Vocab 3000) after the method of Zwank et al. (2003).²² For P&T analysis, the sample was purged for 11 min with helium, (dry purge = 2 min), desorption preheat temperature was 220 °C, and desorption was conducted for 4 min at 225 °C. The trap was baked at 235 °C for 10 min. Isotope $\delta^{13}\text{C}$ values are reported relative to the international V-PDB scale and with a total uncertainty of 0.5‰, incorporating both accuracy and reproducibility.^{6,23} Concentrations in samples for location G–H–I were quite low compared to locations A–B–C and D–E–F. Unfortunately, the combination of low concentrations and small volume (40 mL VOA only) resulted in these being below detection limit for CSIA.

Biofilm Development. Passive samplers can be subject to biofouling on the membrane.²⁴ Significant biofouling could conceivably reduce contaminant mass transfer through the membrane, and/or might contribute to additional contaminant degradation and stable isotope fractionation. To ensure biofilm development and biofouling were not promoted by the peepers, experiments were designed to investigate the potential for intrinsic microbial populations in the site sediments to form a biofilm on top of the peeper polysulfone membrane. Pieces of polysulfone membranes were inserted in field-collected sediments placed in a jar. The jar was left in an anaerobic chamber for 4 weeks. After 4 weeks, the membranes were retrieved, rinsed gently with autoclaved anaerobic buffer solution, and placed in sterile Petri dishes. First, duplicate membrane samples were stained with either a NucBlue Fixed Cell stain or a 4:1 Mounting Medium and DAPI stain. The stained cells were visualized using an Olympus BX51 microscope, and an EXFO X-Cite Series 120Q fluorescence microscope excitation light source. Second, DNA was extracted from triplicate membrane pieces referred to as CA7, CB4, and CA146 with surface areas of 9.2, 10, and 9.3 cm², respectively, using a PowerSoil DNA

isolation kit (Mo Bio Laboratories, Inc.), and following the manufacturer's procedure. DNA was eluted in 50 µL sterile deionized water. DNA was quantified by a NanoDrop ND-1000 spectrophotometer at 260 nm. Results were expressed in ng/cm². Finally, quantitative PCR (qPCR) was conducted to estimate the gene copy numbers of *Dehalobacter*, general archaea, and general bacteria on the membrane biofilm using specific primers: 647r and 477f (*Dehalobacter*),²⁵ 787f and 1059r (archaea), and 1055f and 1392r (bacteria). *Dehalobacter* were specifically targeted because they are known to be the dominant reductive dechlorinators capable of degrading chlorinated benzenes in the sediments of this site.²⁶ Amplification and quantification was done using a Bio-Rad CFX96 Real-Time System with a C1000 Thermal Cycler. Cycling started at 98 °C for 2 min, 39 cycles of 5 s at 98 °C and 10 s at 62.5 °C, and continued by melting curve analysis from 65 to 95 °C. For each of the three groups, the results were expressed as total number of gene copies/cm².

Modeling. The peeper concentration data were modeled by a two-layer steady state advection-diffusion reaction equation accounting for sorption to organic matter. Chemical analysis of solid phase was not done at the time this peeper study was conducted. This was beyond the scope of this work which focuses on a novel application of sediment pore water sampling for CSIA. In the model, K_{oc} values of 224 (MCB) and 98 L/kg (benzene) were used, as shown in Supporting Information (SI) Table S1. A first-order degradation rate was assumed. The model is equivalent to that described by Lampert and Reible (2009).²⁷ Details on the model are provided in SI Section S1. The chloride concentration data were first used to estimate the Darcy pore water velocity. This value was then applied when using the model to estimate MCB and benzene degradation rate constants.

RESULTS

Redox Conditions. Nitrate concentrations were below detection at all depths in the sediment, and maximum concentrations were lower than 1 mg/L in the surface water (Figure 1). Total iron concentrations were also low in the surface water (0.11–2.19 mg/L), but increased in mid-depth profile, with maximum values of 26.0 mg/L 18 cm below the sediment–water interface (b.s.w.i.) (location A–B–C), 26.3 mg/L 18 cm b.s.w.i. (location D–E–F), and 32.2 mg/L 10.5 cm b.s.w.i. (location G–H–I). Total iron concentrations then decreased further down toward the deepest levels sampled, with concentrations ranging from 14.0 to 17.4 mg/L 24 cm deep in the sediment profile. Total iron included both solid and dissolved iron species. Mainly soluble Fe(II), as well as colloid-attached Fe(III) are expected to cross the 0.45 µm peeper membrane. Finally, sulfate concentrations were below detection along most of the sediment profile up to the top 5 cm. Sulfate concentrations were 26.1 mg/L at the sediment–water interface (location A–B–C), 10.1 mg/L 3 cm b.s.w.i. (location D–E–F), and 5.2 mg/L 4.5 cm b.s.w.i. (location G–H–I). Sulfate concentrations were larger in the surface water (28.2–29.0 mg/L), and decreased downward below the sediment–water interface, reaching below detection levels 6 cm b.s.w.i. (location A–B–C), 9 cm b.s.w.i. (location D–E–F), and 10.5 cm b.s.w.i. (location G–H–I). The sharp downward decrease in sulfate concentration at the sediment–water interface was coincident with the rapid increase in iron concentration. The sequence of redox species did not follow the classic thermodynamic ladder, whereby iron(III) is consumed before

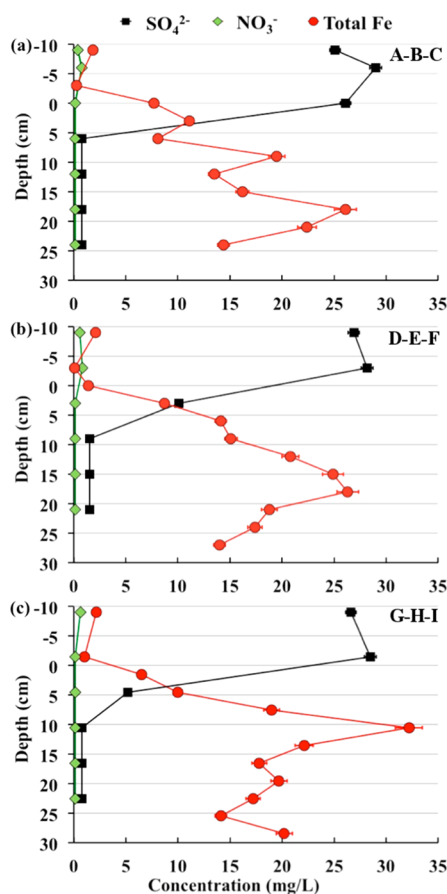


Figure 1. Concentrations of redox species along the sediment profile. Concentrations in mg/L of sulfate (black squares), nitrate (green diamonds), and total iron (red circles) as a function of the depth (cm) across the sediment profile, for locations (a) A–B–C, (b) D–E–F, and (c) G–H–I. The error bars represent the relative percentage differences for sulfate (2%), nitrate (2%), and iron (4%). The error bars on concentrations are often smaller than the symbols. The water–sediment interface is indicated at the depth of 0 cm.

sulfate is reduced.²⁸ However, the pattern detected at the site has been observed often elsewhere^{29–31} and can be associated with high levels of organic matter³⁰ or of available sulfate concentrations.³¹ To distinguish between iron- and sulfate-reducing conditions, Chapelle et al. (2009)³² proposed to compare the ratio of sulfide to iron concentrations to two thresholds: 0.3 and 10. In most locations, the ratios of sulfide concentrations (calculated, see SI Section S2) to iron concentrations were below the threshold of 0.3 in the surface water. Deeper than 6 cm, the ratio was above the threshold of 10. This confirms the dominance of iron reducing conditions across most of the sediment profile, and of sulfate reducing conditions in the surface water near the sediment–water interface.³² These data are a first line of evidence for microbial activity at the water–sediment interface.

Monochlorobenzene and Benzene Concentration Profiles. Monochlorobenzene and benzene were detected at all three peeper locations, with similar concentration profiles (Figure 2). The highest MCB and benzene concentrations were measured in the bottommost layers of the sediment, and showed decreasing upward trends. Maximum MCB concentrations were 2000 (location A–B–C), 720 (location D–E–F), and 300 $\mu\text{g/L}$ (location G–H–I), whereas maximum benzene concentrations were 1 order of magnitude lower: 180, 92, and

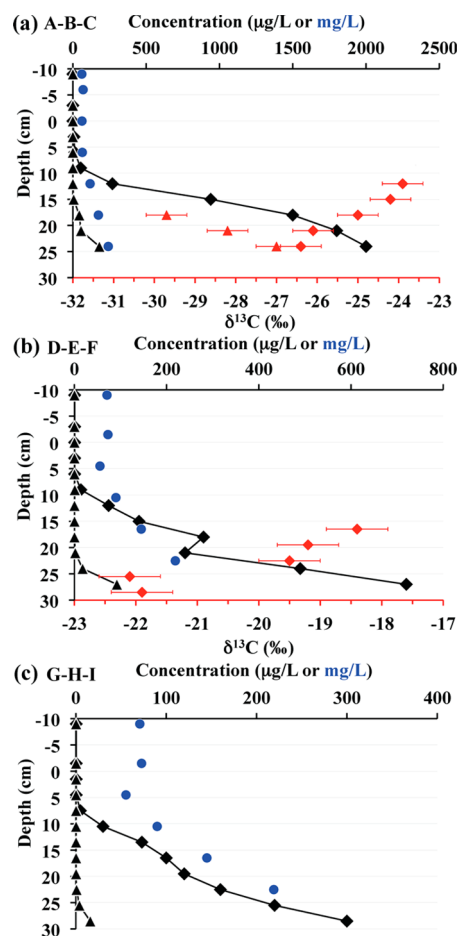


Figure 2. Concentration and stable isotope values of MCB and benzene along the sediment profile. Concentrations of MCB (in $\mu\text{g/L}$, black diamonds), benzene (in $\mu\text{g/L}$, black triangles), chloride (in mg/L , blue circles), and $\delta^{13}\text{C}$ values (in ‰) of MCB (red diamonds) and benzene (red triangles) as a function of the depth (cm) along the sediment profile at locations (a) A–B–C, (b) D–E–F, and (c) G–H–I. The error bars for concentration, representing the relative percentage difference for MCB (1%), benzene (2%), and chloride (2%), are smaller than symbol size. The error bars on $\delta^{13}\text{C}$ values represent a ± 0.5 ‰ total error encompassing both accuracy and reproducibility after Sherwood Lollar et al.²³ Note differences in scales of horizontal axes. The water–sediment interface is placed at a depth of 0 cm. The black lines on MCB and benzene concentration data were drawn to improve figure clarity; they do not represent model fit (see SI Figure S1 for model fit to the data). No $\delta^{13}\text{C}$ values were obtained for benzene and MCB in location G–H–I (c) as benzene and MCB were below CSIA detection limit.

16 $\mu\text{g/L}$, for the respective locations. Concentrations for MCB were below detection in the top 3–9 cm b.s.w.i., whereas, benzene concentrations were undetectable above 15–22.5 cm b.s.w.i. Chloride concentrations were 2 orders of magnitude higher than both MCB and benzene concentrations. This is due to natural background chloride concentrations and the likely release of chloride during anaerobic reductive dechlorination of dichlorobenzenes and trichlorobenzenes present in the groundwater. Therefore, chloride concentrations cannot be reliably used to estimate MCB dechlorination in the sediment. However, they can be considered sufficiently unaffected by MCB-produced chloride to be used in modeling for Darcy velocity estimations.

Modeling Results. The estimated Darcy pore water advection velocities using the chloride data were consistently in the same order of magnitude, with calculated velocities of 5.9 (location A–B–C), 8.4 (location D–E–F), and 9.3 cm/yr (location G–H–I). The positive velocity values indicate that the flow was upward. The MCB and benzene degradation rate constants and half-lives are summarized in Table 1 and Figure

Table 1. Summary of the Concentration Modeling Results

	location	location	location
	A–B–C	D–E–F	G–H–I
U (cm/yr) ^a	5.9	8.4	9.3
MCB			
Top			
k_{top} (yr ⁻¹) ^b	40	4.6	5.3
DT _{50, top} (d) ^c	6.4	55	47
Bottom			
k_{bottom} (yr ⁻¹) ^b	0	4.7	3.0
DT _{50, bottom} (d) ^c		54	84
SSE ^d	17 600	22 500	1570
Benzene			
Bottom			
k_{bottom} (yr ⁻¹) ^b	19	56	42
DT _{50, bottom} (d) ^c	13	4.6	6.0
SSE ^d	488	3	0.3

^aDarcy velocity, obtained by fitting the model to the chloride data at each location. ^b k_{top} and k_{bottom} are the first-order degradation rate constants for the top and bottom layers of the sediment profile, respectively, derived from Lampert and Reible (2009) (See SI Section S1). In the case of benzene, given that all benzene concentrations were below detection in the top layer, k_{top} was set to zero and k_{bottom} only was fitted. ^cDT_{50, bottom} and DT_{50, top} are the half-lives for the bottom and top layers of the sediment profile, respectively. ^dSSE: Total error sum of squares in fitting parameters k_{bottom} and k_{top} .

S1. For MCB, the top layer and bottom layer first-order degradation rate constants for MCB were 40 yr⁻¹ (top) and null (bottom) for location A–B–C, 4.6 (top) and 4.7 yr⁻¹ (bottom) for location D–E–F, and 5.3 (top) and 3.0 yr⁻¹ (bottom) for location G–H–I. The corresponding MCB half-life range was 6.4–55 days (top) and 54–84 days (bottom); whereas, for benzene, half-lives were much shorter, ranging from 4.6 to 13 days in the bottom layer.

Stable Carbon Isotope Values. Consistent with the concentration decreases across the profiles, and the calculated biodegradation rates, stable isotope analysis of MCB confirmed the effects of biodegradation through a clear enrichment trend in ¹³C upward through the sediment profile (Figures 2a and b). In the bottommost peeper interval, the correlation between the highest MCB concentrations and the most depleted isotope values of -26.4 ‰ (location A–B–C), and -21.9 ‰ (location D–E–F) confirm these are the least degraded portions of the profile. The difference of 4.5 ‰ between these two points is consistent with location D–E–F exhibiting lower concentrations (720 μg/L) than location A–B–C (2000 μg/L), likely due to a higher degree of biodegradation for the former compared to the latter. Higher up in the profile, lower MCB concentrations and more enriched ¹³C values for MCB, -23.9 ‰ at 12 cm b.s.w.i. at location A–B–C, and -18.4 ‰ at 16.5 cm b.s.w.i. at location D–E–F, confirm that MCB at these locations was more extensively biodegraded than at the base of the profiles. Enrichments in ¹³C of 2.5 (location A–B–C) and

3.5 ‰ (location D–E–F) were noted between the lowest and highest concentration zones. Due to lower concentrations, benzene ¹³C values were obtained for a smaller number of samples and only for location A–B–C. Nonetheless, this albeit limited ¹³C benzene data set provides an important additional line of evidence for MCB biodegradation across the sediment–water interface. At the lowest depth (24 cm b.s.w.i.) where the highest benzene concentration was measured (180 μg/L), the benzene ¹³C value was -27.0 ‰. In contrast, 18 cm b.s.w.i., where benzene concentration was 43 μg/L a more depleted ¹³C value (-29.7 ‰) was measured. This was likely the result of three simultaneous processes: benzene upward transport from deeper levels, production from MCB dechlorination, and possible further degradation of benzene. At all intervals where both MCB and benzene ¹³C values were obtained, the benzene is always more depleted than the MCB, consistent with what would be expected for a product of MCB biodegradation (Figure 2).

Extent of Biodegradation. One mole of MCB degraded via reductive dechlorination produces one mole of benzene. The expected amount of benzene produced from MCB dechlorination was calculated from two data sets: first, based on MCB concentration differences between two depths, and second, applying a biodegradation factor calculated using MCB isotope values. The results are reported in SI Table S2.

Monochlorobenzene and benzene were both quantified above detection limits in intervals of 15–24 cm b.s.w.i. (location A–B–C), 21–27 cm b.s.w.i. (location D–E–F), and 22.5–28.5 cm b.s.w.i. (location G–H–I). In these intervals, MCB and benzene were not stoichiometrically equivalent: the molar concentration differences were 9.6 (MCB) and 2.2 μmol/L (benzene) for location A–B–C; 4.3 (MCB) and 1.2 μmol/L (benzene) for location D–E–F; and 1.3 (MCB) and 0.2 μmol/L (benzene) for location G–H–I (SI Table S2).

Applying the Rayleigh equation (eq 2) with the measured ¹³C values (-26.4 and -23.9 ‰ for 24 and 12 cm b.s.w.i., respectively), in combination with the isotope enrichment factor for MCB during reductive dechlorination (-5.0 ± 0.2 ‰),³³ an estimate of about 40 % MCB biodegradation was calculated for location A–B–C. Similar results were found for location D–E–F between 16.5 (-18.4 ‰) and 28.5 cm (-21.9 ‰) b.s.w.i. which led to an estimate of about 50 % MCB biodegradation. Applying the estimated percent MCB biodegradation obtained from the isotope results to measured MCB concentrations, and calculating the equivalent benzene concentrations that should be produced from 40 % MCB dechlorination, indicates that observed benzene concentrations were lower than would be predicted (SI Table S2). For example: for location A–B–C, a 200 μg/L MCB concentration difference was measured between the 24 (2000 μg/L) and 21 cm (1800 μg/L) depths. Based on the isotope data, 40 % of this concentration decrease is expected to be due to biodegradation. This suggests that 80 μg/L of MCB was biodegraded between these two depths (i.e., 200 μg/L × 40 %). As one mole of MCB yields one mole of benzene, the equivalent benzene produced from 80 μg/L of dechlorinated MCB in the depth interval is 56 μg/L (80 μg/L × 78.11 g_{benzene}/mol_{benzene}/112.56 g_{MCB}/mol_{MCB}). Adding this value to the 180 μg/L of benzene transported from the 24 cm depth, suggests that 236 μg/L of benzene should have been measured at the 21 cm b.s.w.i. location if benzene itself were not undergoing further degradation. This predicted concentration from transport and MCB biodegradation is much higher than the measured

benzene concentration at that depth (56 $\mu\text{g/L}$), suggesting that in addition to production of benzene from MCB, there must be simultaneous biodegradation of benzene itself in the sediment.

Biofilm Development. In the biofilm laboratory experiments, the site sediments did not appear to produce significant biofilm on the polysulfone membrane. Microscope observations showed no significant accumulation of cells on the membrane pieces that were in contact with the site sediments for 4 weeks. Similarly, for all three membranes, the average DNA concentration was $31.3 \pm 2.4 \text{ ng/cm}^2$, and gene copies for general bacteria ($1.73 \times 10^5 \pm 2.15 \times 10^5$), general archaea ($1.66 \times 10^4 \pm 3.24 \times 10^3$), and *Dehalobacter* spp. ($3.87 \times 10^3 \pm 4.62 \times 10^2$) were small (see SI Section S4, Tables S3 and S4). Given that very limited biofilm developed onto the polysulfone membrane, and in particular, that this biofilm contained insignificant amounts of *Dehalobacter* spp., it is unlikely that membrane biofouling affected contaminant isotope signatures.

DISCUSSION

The field results all support ongoing natural attenuation of MCB in the contaminated sediments. The vertical profile of MCB concentration is consistent with both upward transport of MCB and ongoing biodegradation across the sediment–water interface resulting in below detection (5 $\mu\text{g/L}$) MCB levels in the top 3–9 cm of the sediment profile and the overlying surface water. The redox data suggested the dominance of iron reducing conditions along the bottom portion of the sediment. Such redox conditions are known to support MCB microbial degradation via reductive dechlorination.^{17,34} Both the observed reducing conditions and the presence of benzene with a similar upward concentration decrease as for MCB, suggest that MCB dechlorination is occurring along the sediment profile. The strongest line of evidence is provided by the significant enrichment in ^{13}C in MCB concomitant with decreasing concentrations of MCB. The 2.5 and 3.5 ‰ enrichments in $\delta^{13}\text{C}$ values, for locations A–B–C and D–E–F, respectively, indicate MCB biodegradation likely via reductive dechlorination, as anaerobic MCB biodegradation is associated with enrichment factors on the order of $-5.0 \pm 0.2 \text{ ‰}$.³³ The first-order degradation rate constants (k_{bottom} and k_{top}), and therefore the MCB half-lives, were determined based on concentration data. Values for k_{bottom} and k_{top} were of the same order of magnitude ($3.0\text{--}5.3 \text{ yr}^{-1}$) except for location A–B–C for which the best model fit was obtained for a large k_{top} (40 yr^{-1}) compared to a null k_{bottom} . In laboratory experiments conducted with sediments collected at the same site but at a different location, Kurt et al. (2012, 2013)^{35,36} showed that the water–sediment interface was a highly microbially active zone for MCB degradation. Measured degradation rates in column experiments under anaerobic conditions were $21 \pm 1 \text{ mg}_{\text{MCB}} \cdot \text{m}^{-2} \cdot \text{d}^{-1}$ for a flow rate of $2 \text{ mL} \cdot \text{h}^{-1}$ (equivalent to more than $30\,000 \text{ cm/yr}$).³⁵ The flow rate selected in this lab experiment was 4 orders of magnitude higher than the field Darcy velocity of 5.9–9.3 cm/yr estimates in this study. The microbes in the top portion of the sediment profile likely played a significant role resulting in complete MCB removal. *Dehalobacter* spp. was shown to be responsible for MCB dehalogenation to benzene³⁷ in sediment microcosms³⁸ and enrichment cultures.²⁶ With the field results presented herein, and MCB half-life ranging from 6.4 to 84 days, these results demonstrate that the ongoing in situ natural attenuation of MCB was sufficient to protect the overlying surface water.

Benzene $\delta^{13}\text{C}$ values observed were always more depleted than those of MCB for each interval, consistent with the expectations if benzene is produced by biodegradation of MCB, and suggesting a significant component of the observed benzene was produced from MCB by reductive dechlorination.

As for MCB, the highest benzene concentrations were at the bottom of the sediment profile, and concentrations decreased upward. Benzene concentrations were 1–2 orders of magnitude lower than MCB concentrations, and were below detection limits by 15–22.5 cm b.w.s.i., demonstrating that the overlying water is protected by the biologically active zone at the sediment–water interface. The source of MCB and benzene at this location is groundwater discharge from the site. Concentrations of MCB and benzene in the surface water were below detection limits, however. This indicates that new sediments from the canal water deposited on top of the profiles are unlikely to contain contaminants. Benzene isotope $\delta^{13}\text{C}$ values became progressively more depleted in ^{13}C while concentrations decreased (Figure 2). Anaerobic biodegradation of benzene produces isotopic fractionation, although with a smaller range of enrichment factors ($-1.9 \pm 0.1 \text{ ‰}$ to $-3.6 \pm 0.3 \text{ ‰}$ ^{39,40}) compared to MCB dechlorination ($-5.0 \pm 0.2 \text{ ‰}$ ³³). Though this field study cannot provide definitive evidence for benzene biodegradation, the absence of stoichiometry between benzene and MCB, and the ^{13}C -depleted benzene $\delta^{13}\text{C}$ values are likely the result of three simultaneous processes: transport upward from groundwater, production of benzene from MCB dechlorination, and anaerobic biodegradation of benzene to CO_2 and CH_4 .

This hypothesis is supported by previous results for sediment microcosms from the same site that were bioaugmented under sulfate reducing condition with a mixed culture containing a *Dehalobacter* spp.-enriched MCB-degrading culture derived from the study site, and a benzene degrading culture.³⁷ Though the benzene-degrading culture added in this laboratory experiment has not been reported at the site, the study nonetheless demonstrates the potential for complete MCB and benzene anaerobic biodegradation to CO_2 and CH_4 . In addition, it was shown that electrons derived from benzene fermentation (benzene $\rightarrow \text{CO}_2/\text{CH}_4$) could be used, in the absence of other electron donors, to fuel MCB reductive dechlorination.³⁷ As benzene can also biodegrade anaerobically under iron reducing conditions,⁴¹ it is reasonable to expect a similar production of benzene from MCB and its further conversion to CO_2 and CH_4 at the site.

Implications for Monitored Natural Attenuation in Contaminated Sediments. There were several key findings in this study. First, the pore water in the biologically active zone of the sediment—the most important route of exposure to benthic organisms³—had MCB and benzene concentrations below detection levels, thus reducing the risk of contaminant transfer to the food web at the site.

Second, the combined use of peepers and CSIA provided a direct line of evidence for in situ MCB dechlorination within the sediment profile at fine spatial resolution. The $\delta^{13}\text{C}$ values of both MCB and benzene supported this conclusion. The lowest MCB concentrations were associated with the most enriched in ^{13}C isotope values within each sediment profile, as well as between the different peeper locations. The more depleted benzene $\delta^{13}\text{C}$ values compared to those of MCB are consistent with a significant contribution to the benzene pool due to dechlorination of MCB. These isotope results confirm that the MCB concentration profile observed in the sediment–

water interface was not simply due to advective–diffusive transport, sorption, and physical processes of contaminant transport and distribution, but involved a very important reduction due to microbial degradation and transformation as well.

Third, the sampling design of this field study helped clarify the origin of benzene. As mentioned above, benzene $\delta^{13}\text{C}$ values were more depleted than those of MCB, confirming its production from MCB reductive dechlorination within the sediment profile. It is also likely that some groundwater benzene was transported upward in the sediment. The molar balance analysis and stable carbon isotope signatures, and the high resolution vertical profiles produced for MCB and benzene were essential for demonstrating the biodegradation of MCB, and the simultaneous transport, production, and biodegradation processes that control benzene fate and transport across the sediment–water interface.

The main implication of these results is that, although CSIA is most commonly used to monitor natural attenuation of contaminated aquifers, its application to peeper-collected sediment pore water can provide key insights into the progress of remediation. This study is the first to propose a method for a successful application of CSIA to MNR of contaminated sediments. With hundreds of contaminated sediment sites across the world, this peeper-CSIA technique has potential to help site managers in monitoring the recovery of contaminated sediment sites due to either natural processes or enhanced remediation. This technique can facilitate decision-making in identifying the site remediation approaches providing the highest chances of success while minimizing cost.

■ ASSOCIATED CONTENT

📄 Supporting Information

The Supporting Information is available free of charge on the ACS Publications website at DOI: 10.1021/acs.est.6b02961.

Details on the model (Section S1), redox species (Section S2), mass balances (Section S3), and biofilm experiments (Section S4) (PDF)

■ AUTHOR INFORMATION

Corresponding Author

*Phone: 001 416 978 5747; fax: 001 416 978 6813; e-mail: elodie.passeport@utoronto.ca.

Present Addresses

[#](E.P.) Department of Civil Engineering, University of Toronto, Toronto, M5S 1A4, Canada.

[○](E.P.) Department of Chemical Engineering and Applied Chemistry, University of Toronto, Toronto, M5S 3E5, Canada.

[▽](R.L.) RichLand Consulting LLC, Lincoln University, Pennsylvania, 19352, United States.

Notes

The authors declare no competing financial interest.

■ ACKNOWLEDGMENTS

We thank Luz A. Puentes Jácome for help in microbial analyses and microscope observation for the biofilm experiments. The research was funded by a grant from DuPont Canada and a Collaborative Research and Development grant from the Natural Science and Engineering Research Council of Canada to B. Sherwood Lollar.

■ REFERENCES

- (1) USEPA. *The Incidence and Severity of Sediment Contamination in Surface Waters of the United States, National Sediment Quality Survey*, 2nd ed., EPA-823-R-04-007; United States Environmental Protection Agency, 2004; p 280. <https://nepis.epa.gov/Exe/ZyPURL.cgi?Dockey=901U0000.txt>.
- (2) USEPA. *EPA's Contaminated Sediment Management Strategy*, EPA-823-R-98-001; United States Environmental Protection Agency, Office of Water 4305: United States Environmental Protection Agency, Office of Water 4305, 1998; p 131. <https://nepis.epa.gov/Exe/ZyPURL.cgi?Dockey=20003Z7X.txt>.
- (3) USEPA. *Contaminated Sediment Remediation Guidance for Hazardous Waste Sites*, EPA-540-R-05-012 OSWER 9355.0-85; United States Environmental Protection Agency, Office of Solid Waste and Emergency Response: United States Environmental Protection Agency, Office of Solid Waste and Emergency Response, 2005. <https://nepis.epa.gov/Exe/ZyPURL.cgi?Dockey=P1000R7F.txt>.
- (4) Santschi, P.; Hohener, P.; Benoit, G.; Buchholtzenbrink, M. Chemical processes at the sediment water interface. *Mar. Chem.* **1990**, *30* (1–3), 269–315.
- (5) USDOD Technical guide: monitored natural recovery at contaminated sediment sites, ESTCP Project ER-0622; 2009. <https://clu-in.org/download/contaminantfocus/sediments/ER-0622-MNR-FR.pdf>.
- (6) Hunkeler, D.; Meckenstock, R. U.; Sherwood Lollar, B.; Schmidt, T. C.; Wilson, J. T. A *Guide for Assessing Biodegradation and Source Identification of Organic Ground Water Contaminants Using Compound Specific Isotope Analysis (CSIA)*; United States Environmental Protection Agency, Ada, OK, 2008; p 67 pp. <https://nepis.epa.gov/Exe/ZyPURL.cgi?Dockey=P1002VAL.txt>.
- (7) Passeport, E.; Landis, R.; Mundle, S. O.; Chu, K.; Mack, E. E.; Lutz, E.; Sherwood Lollar, B. Diffusion sampler for compound specific carbon isotope analysis of dissolved hydrocarbon contaminants. *Environ. Sci. Technol.* **2014**, *48* (16), 9582–9590.
- (8) Slater, G. F.; Ahad, J. M. E.; Sherwood Lollar, B.; Allen-King, R.; Sleep, B. Carbon isotope effects resulting from equilibrium sorption of dissolved VOCs. *Anal. Chem.* **2000**, *72* (22), 5669–5672.
- (9) Harrington, R. R.; Poulson, S. R.; Drever, J. I.; Colberg, P. J. S.; Kelly, E. F. Carbon isotope systematics of monoaromatic hydrocarbons: vaporization and adsorption experiments. *Org. Geochem.* **1999**, *30* (8A), 765–775.
- (10) Poulson, S. R.; Drever, J. I. Stable isotope (C, Cl, and H) fractionation during vaporization of trichloroethylene. *Environ. Sci. Technol.* **1999**, *33* (20), 3689–3694.
- (11) Slater, G. F.; Dempster, H. S.; Sherwood Lollar, B.; Ahad, J. Headspace analysis: A new application for isotopic characterization of dissolved organic contaminants. *Environ. Sci. Technol.* **1999**, *33* (1), 190–194.
- (12) Dempster, H. S.; Sherwood Lollar, B.; Feenstra, S. Tracing organic contaminants in groundwater: A new methodology using compound-specific isotopic analysis. *Environ. Sci. Technol.* **1997**, *31* (11), 3193–3197.
- (13) Elsner, M.; Lacrampe-Couloume, G.; Mancini, S.; Burns, L.; Sherwood Lollar, B. Carbon isotope analysis to evaluate nanoscale Fe(0) treatment at a chlorohydrocarbon contaminated site. *Groundwater Monit. Rem.* **2010**, *30* (3), 79–95.
- (14) Mancini, S. A.; Lacrampe-Couloume, G.; Jonker, H.; Van Breukelen, B. M.; Groen, J.; Volkering, F.; Sherwood Lollar, B. Hydrogen isotopic enrichment: An indicator of biodegradation at a petroleum hydrocarbon contaminated field site. *Environ. Sci. Technol.* **2002**, *36* (11), 2464–2470.
- (15) Sherwood Lollar, B.; Slater, G. F.; Sleep, B.; Witt, M.; Klecka, G. M.; Harkness, M.; Spivack, J. Stable carbon isotope evidence for intrinsic bioremediation of tetrachloroethene and trichloroethene at area 6, Dover Air Force Base. *Environ. Sci. Technol.* **2001**, *35* (2), 261–269.
- (16) Griebler, C.; Safinowski, M.; Vieth, A.; Richnow, H. H.; Meckenstock, R. U. Combined application of stable carbon isotope analysis and specific metabolites determination for assessing in situ

degradation of aromatic hydrocarbons in a tar oil-contaminated aquifer. *Environ. Sci. Technol.* **2004**, *38* (2), 617–631.

(17) Braeckelvel, M.; Rokadia, H.; Imfeld, G.; Stelzer, N.; Paschke, H.; Kuschik, P.; Kaestner, M.; Richnow, H.-H.; Weber, S. Assessment of in situ biodegradation of monochlorobenzene in contaminated groundwater treated in a constructed wetland. *Environ. Pollut.* **2007**, *148* (2), 428–437.

(18) Slater, G. F. Carbon cycling in the microbial mats and bottom accumulations of selected lakes of the Cariboo Plateau: isotopic constraints and implications for interpretation of the geologic record. M.A.Sc. Dissertation, University of Toronto, Toronto, ON, Canada, 1997.

(19) Slater, G. F.; Cowie, B. R.; Harper, N.; Droppo, I. G. Variation in PAH inputs and microbial community in surface sediments of Hamilton Harbour: Implications to remediation and monitoring. *Environ. Pollut.* **2008**, *153* (1), 60–70.

(20) Morrill, P. L.; Szponar, N.; Johnston, M.; Marvin, C.; Slater, G. F. Deciphering microbial carbon substrates in PAH contaminated sediments using phospholipid fatty acids, and compound specific $\delta^{13}\text{C}$ and $\Delta^{14}\text{C}$. *Org. Geochem.* **2014**, *69*, 76–87.

(21) Liu, K.; Wu, L.; Couture, R.-M.; Li, W.; Van Cappellen, P. Iron isotope fractionation in sediments of an oligotrophic freshwater lake. *Earth Planet. Sci. Lett.* **2015**, *423*, 164–172.

(22) Zwank, L.; Berg, M.; Schmidt, T. C.; Haderlein, S. B. Compound-specific carbon isotope analysis of volatile organic compounds in the low-microgram per liter range. *Anal. Chem.* **2003**, *75* (20), 5575–5583.

(23) Sherwood Lollar, B.; Hirschorn, S. K.; Chartrand, M. M. G.; Lacrampe-Couloume, G. An approach for assessing total instrumental uncertainty in compound-specific carbon isotope analysis: Implications for environmental remediation studies. *Anal. Chem.* **2007**, *79* (9), 3469–3475.

(24) ITRC. *Technology Overview of Passive Sampler Technologies*; The Interstate Technology & Regulatory Council Diffusion Sampler Team, 2006; p 115. http://www.itrcweb.org/GuidanceDocuments/DSP_4.pdf.

(25) Grostern, A.; Edwards, E. A. Characterization of a dehalobacter coculture that dechlorinates 1,2-dichloroethane to ethene and identification of the putative reductive dehalogenase gene. *Appl. Environ. Microb.* **2009**, *75* (9), 2684–2693.

(26) Nelson, J. L.; Fung, J. M.; Cadillo-Quiroz, H.; Cheng, X.; Zinder, S. H. A role for dehalobacter spp. in the reductive dehalogenation of dichlorobenzenes and monochlorobenzene. *Environ. Sci. Technol.* **2011**, *45* (16), 6806–6813.

(27) Lampert, D. J.; Reible, D. An analytical modeling approach for evaluation of capping of contaminated sediments. *Soil Sediment Contam.* **2009**, *18* (4), 470–488.

(28) Bethke, C. M.; Sanford, R. A.; Kirk, M. F.; Jin, Q.; Flynn, T. M. The thermodynamic ladder in geomicrobiology. *Am. J. Sci.* **2011**, *311* (3), 183–210.

(29) Cozzarelli, I. M.; Herman, J. S.; Baedecker, M. J.; Fischer, J. M. Geochemical heterogeneity of a gasoline-contaminated aquifer. *J. Contam. Hydrol.* **1999**, *40* (3), 261–284.

(30) Baez-Cazull, S.; McGuire, J. T.; Cozzarelli, I. M.; Raymond, A.; Welsh, L. Centimeter-scale characterization of biogeochemical gradients at a wetland-aquifer interface using capillary electrophoresis. *Appl. Geochem.* **2007**, *22* (12), 2664–2683.

(31) Blodau, C.; Hoffmann, S.; Peine, A.; Peiffer, S. Iron and sulfate reduction in the sediments of acidic mine lake 116 (Brandenburg, Germany): Rates and geochemical evaluation. *Water, Air, Soil Pollut.* **1998**, *108* (3–4), 249–270.

(32) Chapelle, F. H.; Bradley, P. M.; Thomas, M. A.; McMahon, P. B. Distinguishing iron-reducing from sulfate-reducing conditions. *Groundwater* **2009**, *47* (2), 300–305.

(33) Liang, X.; Howlett, M. R.; Nelson, J. L.; Grant, G.; Dworatzek, S.; Lacrampe-Couloume, G.; Zinder, S. H.; Edwards, E. A.; Sherwood Lollar, B. Pathway-dependent isotope fractionation during aerobic and anaerobic degradation of monochlorobenzene and 1,2,4-trichlorobenzene. *Environ. Sci. Technol.* **2011**, *45* (19), 8321–8327.

(34) Schmidt, M.; Wolfram, D.; Birkigt, J.; Ahlheim, J.; Paschke, H.; Richnow, H.-H.; Nijenhuis, I. Iron oxides stimulate microbial monochlorobenzene in situ transformation in constructed wetlands and laboratory systems. *Sci. Total Environ.* **2014**, *472*, 185–193.

(35) Kurt, Z.; Spain, J. C. Biodegradation of chlorobenzene, 1,2-dichlorobenzene, and 1,4-dichlorobenzene in the vadose zone. *Environ. Sci. Technol.* **2013**, *47* (13), 6846–6854.

(36) Kurt, Z.; Shin, K.; Spain, J. C. Biodegradation of chlorobenzene and nitrobenzene at interfaces between sediment and water. *Environ. Sci. Technol.* **2012**, *46* (21), 11829–11835.

(37) Liang, X.; Devine, C. E.; Nelson, J.; Sherwood Lollar, B.; Zinder, S.; Edwards, E. A. Anaerobic conversion of chlorobenzene and benzene to CH₄ and CO₂ in bioaugmented microcosms. *Environ. Sci. Technol.* **2013**, *47* (5), 2378–2385.

(38) Fung, J. M.; Weisenstein, B. P.; Mack, E. E.; Vidumsky, J. E.; Ei, T. A.; Zinder, S. H. Reductive dehalogenation of dichlorobenzenes and monochlorobenzene to benzene in microcosms. *Environ. Sci. Technol.* **2009**, *43* (7), 2302–2307.

(39) Mancini, S. A.; Ulrich, A. C.; Lacrampe-Couloume, G.; Sleep, B.; Edwards, E. A.; Sherwood Lollar, B. Carbon and hydrogen isotopic fractionation during anaerobic biodegradation of benzene. *Appl. Environ. Microb.* **2003**, *69* (1), 5191–5194.

(40) Fischer, A.; Herklotz, L.; Herrmann, S.; Thullner, M.; Weelink, S. A. B.; Stams, A. J. M.; Schlömann, M.; Richnow, H.-H.; Vogt, C. Combined carbon and hydrogen isotope fractionation investigations for elucidating benzene biodegradation pathways. *Environ. Sci. Technol.* **2008**, *42* (12), 4356–4363.

(41) Lovley, D. R. Anaerobic benzene degradation. *Biodegradation* **2000**, *11* (2–3), 107–116.